International Journal of Multiphysics
Volume 18, No. 1s, 2024
ISSN: 1750-9548

Influence of Impact Angle and Thickness on Deformation of Axially Compressed Aluminum Square Tube

Itsuki MARUYAMA, Makoto MIYAZAKI*, Akifumi KARASAWA
National Institute of Technology, Nagano College, Japan
*Corresponding author miyazaki@nagano-nct.ac.jp

Abstract

Aluminum tubes are efficient energy absorbing components and are widely used for frameworks and reinforcement members of the structures. The effect of the axial length, cross-sectional shape and impact angle of weight on the deformation behavior were investigated. Regarding the axial length, it has changed only to a certain length, and there are few studies on it. In addition, there are few studies on the effect of aluminum square tube thickness. It is known that when the aluminum square tube is deformed, elastic deformation occurs in the entire square tube prior to plastic deformation. Since this is periodic and wavy, it seems that the axial length will have a large influence. This paper deals with the influence of impact angle on deformation of axially compressed aluminum square tube. An analysis of the dynamic deformation process of the square tube was made with a finite element method. The results shows that when the thickness of the square tube increases, the overall buckling tends to occur as the axial length increases. In addition, when the impact angle increased, there was a tendency for local deformation to occur easily.

1. INTRODUCTION

Square tubes have been used for framework and reinforcement members of structures. There are many studies on circular tubes, and deformation behaviors have been studied by static and dynamic compression tests [1, 2]. Previous studies have shown that square tubes have a role of absorbing impact energy by crushing under pressure in the axial direction at the time of a impact [3, 4]. Aluminum alloy has a Young's modulus that is one-third that of commonly used steel materials, giving it the disadvantage of low rigidity. In addition, the whole buckles become large when thickness is increased, and causing axial compression deformation, which cannot effectively absorb impact energy [5]. The tubular bodies with polygonal tubes and cellular cross sections have been studied as a means to effectively absorb energy [6]. Additionally, an influence of axial length on dynamic axially compressed aluminum tubes is being considered [7-10]. The dynamic axial compression behavior of various kinds of polygonal tubular structures with ribs are considered [11, 12]. It is known that elastic deformation occurs in the entire square tube prior to plastic deformation when the square tube deforms. Since this is periodic and wavy, it seems that the axial length will have a large influence [13]. The purpose of this paper is to discuss the deformation behavior of aluminum square tubes during dynamic axial compression for different axial lengths, impact angles and thicknesses.

2. Numerical Analysis

The analysis is conducted using a nonlinear structure analysis program (Marc 2023) and pre-post processor (Mentat 2023). An example of analytical model is shown in Figure 1. The specimen is an aluminum tube (A6063-T5). The material properties of the tube being analyzed are shown in Table 1. The axial lengths are l = 100 mm, 150 mm, 200 mm, 300 mm and 500 mm. They are discretized with bilinear 4-node shell elements of 4000, 6000, 8000, 12000 and 20000, respectively. The thicknesses of the square tubes are 1 mm, 1.5 mm and 2 mm. In the analysis, an impact angle of θ = 0°, 0.5°, 1°, 1.5°, 2°, 3°, 5° and 10° was given between the weight and the impact edge of the square tube. Schematic diagram of the analysis model is shown in Figure 2.

https://doi.org/10.52710/ijm.v18.i1s.983

International Journal of Multiphysics
Volume 18, No. 1s, 2024
ISSN: 1750-9548

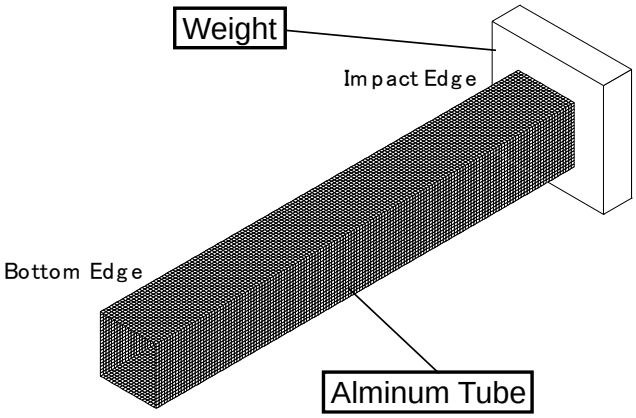

Figure 1: Analytical model of square tube.

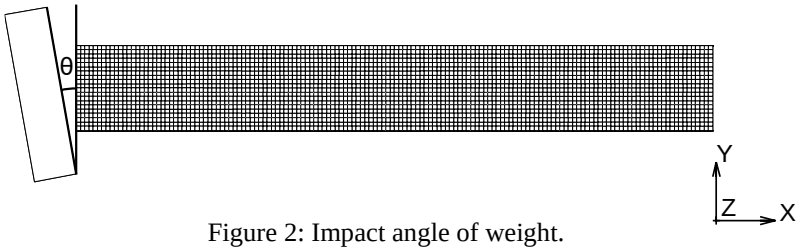

Figure 2: Impact angle of weight.

The nodes at the edge of the tube are fixed with the exception of an axial direction of the impact edge. The weight (80 × 80 × 20 mm, 15 kg) is an un-discretized three-dimensional, eight-node, first-order, isoparametric element. The deformed tube is regarded as an isotropic material following von-Mises yield condition, and the flow stress-strain relationship is described in Equation (1) because the effect of the strain rate of the aluminum is smaller than that of other materials such as iron, etc. [14].

Table 1 Material properties of aluminum (JIS A6063-T5)

Young's modulus	E / GPa	69
Poisson's ratio	v	0.33
Density	ρ / kg/m^3	2.71×10^3
Work-hardening modulus	F / MPa	268
Work-hardening exponent	n	0.065

$$\sigma = F\varepsilon^n . \quad (1)$$

In this analysis, the time step width is 1 μs. The Newton-Raphson method and the updated Lagrangian formulation are used as the solution methods of the non-linear equation, and the single-step Houbolt of implicit solution time-integration method is used for the analysis of dynamic deformation [15]. The impact velocity is 10 m/s.

3. Results

3.1. Analytical results

Final deformations of square tube are shown in Figure 3. When the thickness of the square tube is 1 mm, the deformation shape was concave-convex in adjoining surfaces, and crushed in a bellows-like manner. The square tube is effective for impact absorption member because the impact is absorbed by the partial buckling. On the other hand, when the thickness of the square tube is 1.5 mm, the deformed shape is an overall buckling shape when the axial length is 300 mm and the impact angle is 1° and when the axial length is 500 mm and the impact

angle is 1°. The square tubes are not effective as impact absorbers because the whole square tube is bending and the impact is not absorbed by the partial buckling. Similarly, when the thickness of the square tube is 2 mm, the deformation shape is an overall buckling shape when the axial length is 300 mm and impact angles are 1°, 1.5° and 2° and when the axial length is 500 mm and impact angles are 0.5°, 1°, 1.5° and 2°. It is not effective as an impact absorbing member.

(a)

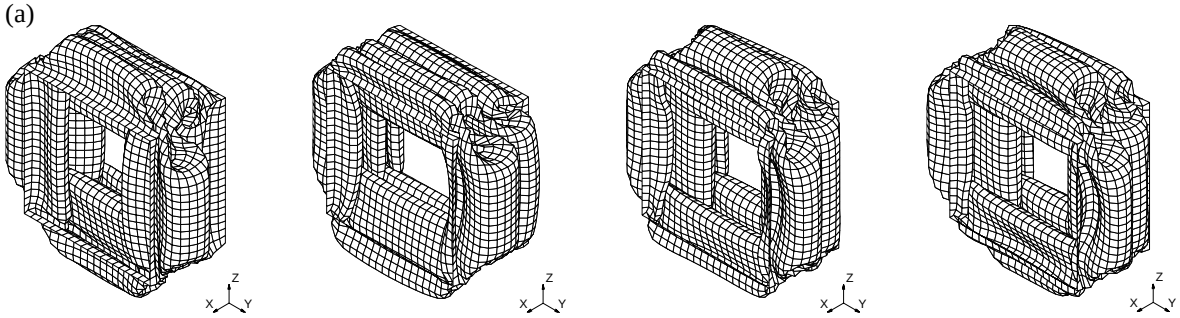

0° 1° 3° 5°

(b)

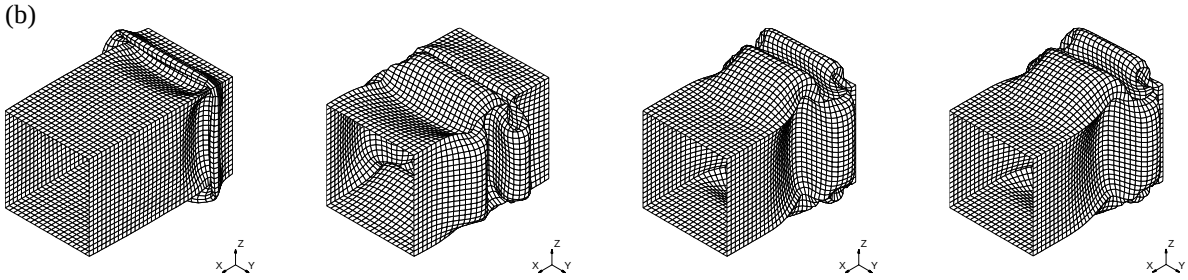

0° 1° 3° 5°

(c)

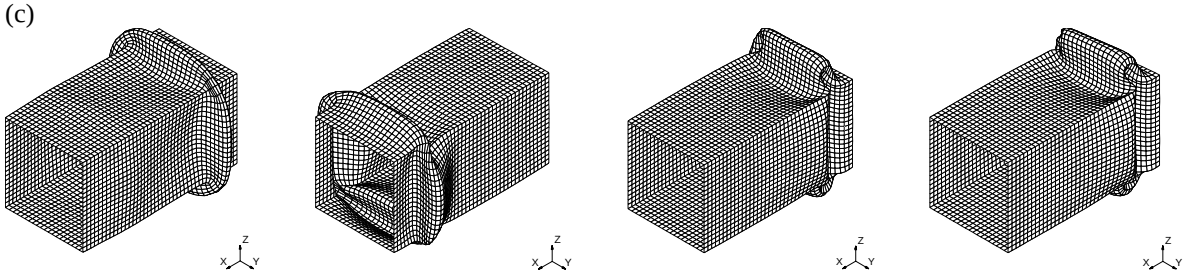

0° 1° 3° 5°

(d)

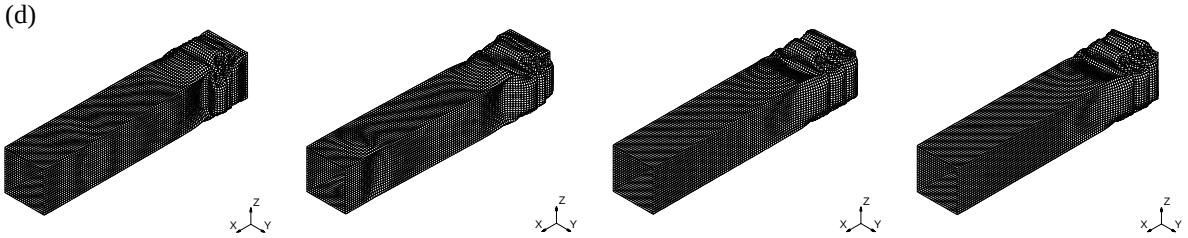

0° 1° 3° 5°

(e)

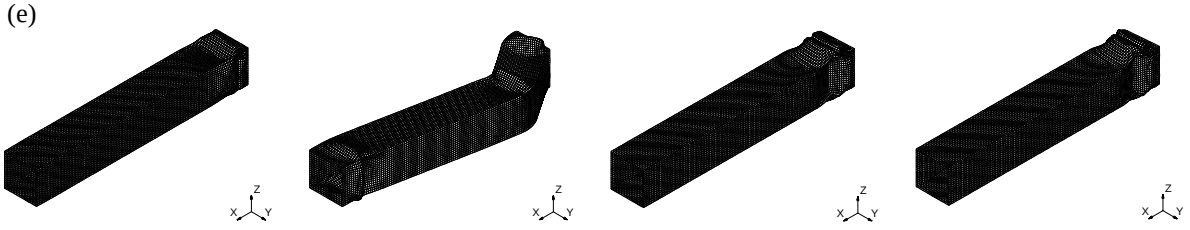

0° 1° 3° 5°

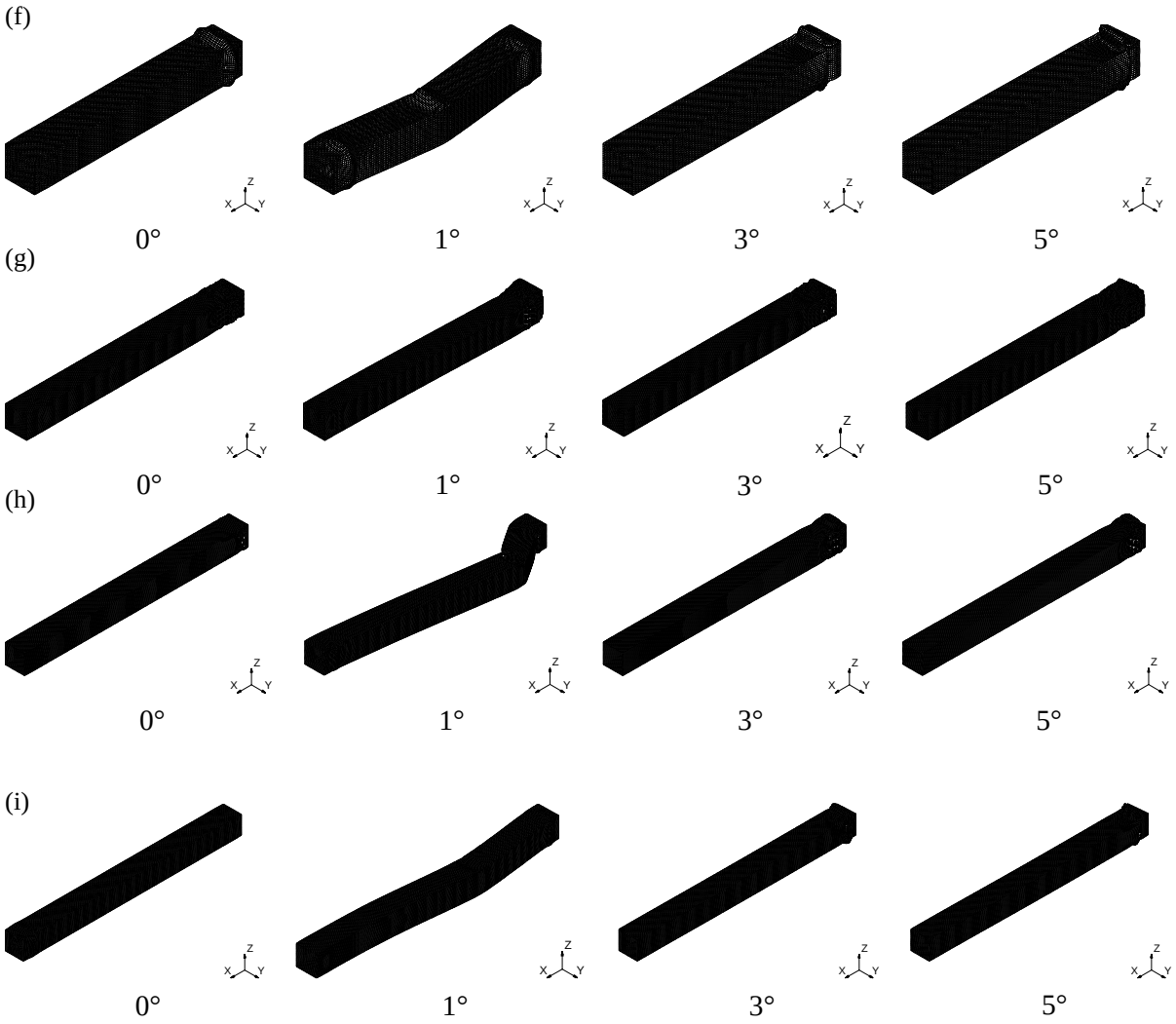

Figure 3: Final deformations of square tube. (a) t = 1mm, l = 100 mm, (b) t = 1.5 mm, l = 100 mm, (c) t = 2 mm, l = 100 mm, (d) t = 1mm, l = 300 mm, (e) t = 1.5 mm, l = 300 mm, (f) t = 2 mm, l = 300 mm, (g) t = 1 mm, l = 500 mm, (h) t = 1.5 mm, l = 500 mm and (i) t = 2 mm, l = 500 mm.

3.2. Strain distribution

Strain distributions along the hill and valley of the concave-convex surface for the case of t = 1 mm, l = 500 mm is shown in Figure 4. Axial Strain around the corners is large regardless of the change in impact angle. Even if the impact angle changes, the trends of the axial strain distribution were not considerably affected. Similar trends are observed at other axial lengths when the thickness of the square tube was 1 mm.

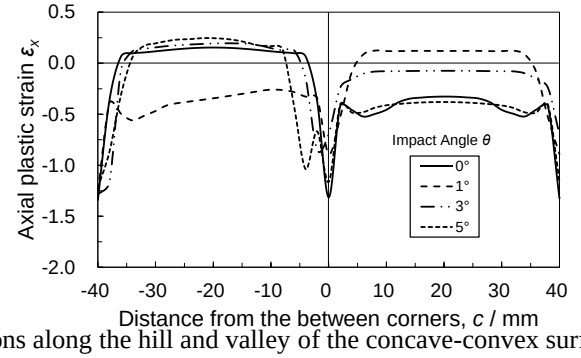

Figure 4: Strain distributions along the hill and valley of the concave-convex surface (t = 1 mm, l = 500 mm).

On the other hand, the strain distribution along the peaks and valleys of the concavo-convex surface for t = 1.5 mm, l = 500 mm and θ = 1° is shown in Figure 5. The strain on one side is almost zero. This is because the whole square tube is bending and the impact is not absorbed by the partial buckling. The same tendency is observed when the thickness of the square tube is 1.5 mm, the axial length is 300 mm and the impact angle is 1° and when the axial length is 500 mm and the impact angle is 1° and when the thickness of the square tube is 2 mm, the axial length is 300 mm and impact angles are 1°, 1.5° and 2° and when the axial length is 500 mm and impact angles are 0.5°, 1°, 1.5° and 2°, because the square tube absorbs the impact by bending.

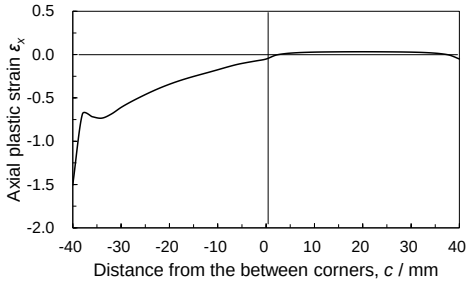

Figure 5: Strain distributions along the hill and valley of the concave-convex surface (t = 1.5 mm, l = 500 mm, θ = 1°).

3.3 Relationship between axial load and Impact angle

Relationship between axial load and impact angle for the case of l = 500 mm and t = 1 mm is shown in Figure 6. When the impact angle of the weight increases beyond a certain angle, the initial peak load becomes smaller. The same tendency is observed for other axial lengths and wall thicknesses. When the impact angle increases, it is conceivable that the time for the upper edge of the square tube to contact the weight is delayed.

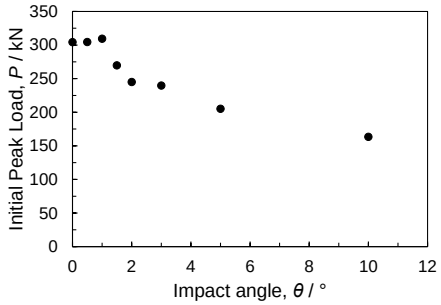

Figure 6: Relationship between axial load and impact angle (l = 500 mm, t = 1mm).

3.4. Relationship between axial displacement and Impact angle

Relationship between axial displacement and Impact angle for the case of l = 500 mm and t = 1mm is shown in Figure 7. When the impact angle of the weight increases beyond a certain angle, the axial displacement tends to increase when the initial peak load occurs. The same tendency is observed for other axial lengths and wall thicknesses.

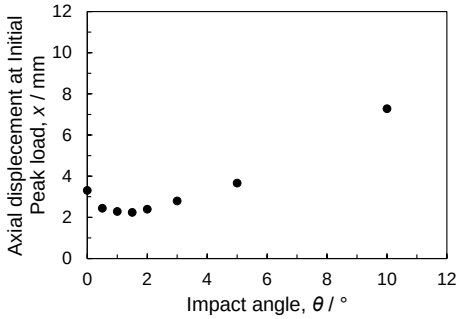

Figure 7: Relationship between axial displacement and impact angle (l = 500 mm, t = 1mm).

4. CONCLUSION

From numerical analysis, the following conclusions were obtained.

(1) When the impact angle of the weight is small, the energy is absorbed by the entire edge, resulting in a larger initial peak load.
(2) When the impact angle of the weight is large, energy is absorbed step by step from the first edge to the second edge, resulting in a smaller initial peak load.
(3) When the impact angle of the weight is large, the axial displacement at the initial peak load is large.
(4) When the thickness of the square tube increases, the overall buckling tends to occur as the axial length increases.
(5) When the impact angle increased, there is a tendency for local deformation to occur easily.

REFERENCES

[1] J. M. Alexander: Q. J. Mech. Appl. Math., 1960, 13: 10-15.

[2] W. Abramowicz and N. Jones, International J. Impact Eng., 1984, 2(2): 179-208.

[3] M. Yamashita, H. Kenmotsu and T. Hattori: Thin-Walled Struct., 2013, 69: 45-53.

[4] J. Fleischer, G. Lanza, S. Dosch, J. Elser and W. Pangboonyanon: Proc. CIRP, 2014, 18: 221-225.

[5] D-K. Kim, S. Lee and M. Rhee, Materials & Design, 1998, 19(4): 179-185.

[6] J Fang, Y. Gao, G. Sun, N. Qiu. and Q. Li: Thin-Walled Struct., 2015, 95: 115-126.

[7] M. Miyazaki, H. Endo, and H. Negishi, J. Mater. Process. Technol., 1999, 85(1-3): 213-216.

[8] M. Miyazaki and H. Negishi, Materials Transactions, 2003, 44(8): 1566-1570.

[9] M. Miyazaki and M Yamaguchi, Procedia Eng., 2014, 81: 1067-1072.

[10] Y. Shinshi, M. Miyazaki, and Keisuke Yokoya: Materials Research Proc., 2019, 13: 41-46.

[11] K. Yokoya, M. Miyazaki, Y. Tojo and M. Yamashita: Procedia Eng., 2017, 207: 251-256.

[12] K. Yokoya, M. Miyazaki, Y. Tojo and M. Yamashita: J. The Japan Institute of Light Metals, 2019, 69(8): 379–386.

[13] S. P. Timoshenko: Theory of Elastic Stability, McGraw-Hill, New York, 1936: 327-333.

[14] S. Tanimura, H. Hayashi, T.Yamamoto and K. Mimura, J. Solid Mech. & Mater., 2009, 3(12): 1263-1273.

[15] J. Chung and G.M. Hulber: Comp. Meth. in App. Mech. Eng., 1994, 118: 1-11.